

Soft Matter

Accepted Manuscript



This is an *Accepted Manuscript*, which has been through the Royal Society of Chemistry peer review process and has been accepted for publication.

Accepted Manuscripts are published online shortly after acceptance, before technical editing, formatting and proof reading. Using this free service, authors can make their results available to the community, in citable form, before we publish the edited article. We will replace this *Accepted Manuscript* with the edited and formatted *Advance Article* as soon as it is available.

You can find more information about *Accepted Manuscripts* in the [Information for Authors](#).

Please note that technical editing may introduce minor changes to the text and/or graphics, which may alter content. The journal's standard [Terms & Conditions](#) and the [Ethical guidelines](#) still apply. In no event shall the Royal Society of Chemistry be held responsible for any errors or omissions in this *Accepted Manuscript* or any consequences arising from the use of any information it contains.

Modeling Tensorial Conductivity of Particle Suspension Networks

Tyler Olsen^a and Ken Kamrin^{*a}

Received Xth XXXXXXXXXXXX 20XX, Accepted Xth XXXXXXXXXXXX 20XX

First published on the web Xth XXXXXXXXXXXX 20XX

DOI: 10.1039/b000000x

Significant microstructural anisotropy is known to develop during shearing flow of attractive particle suspensions. These suspensions, and their capacity to form conductive networks, play a key role in flow-battery technology, among other applications. Herein, we present and test an analytical model for the tensorial conductivity of attractive particle suspensions. The model utilizes the mean fabric of the network to characterize the structure, and the relationship to the conductivity is inspired by a lattice argument. We test the accuracy of our model against a large number of computer-generated suspension networks, based on multiple in-house generation protocols, giving rise to particle networks that emulate the physical system. The model is shown to adequately capture the tensorial conductivity, both in terms of its invariants and its mean directionality.

Introduction

The electrical conductivity of heterogeneous materials has been extensively studied by many different researchers over the years^{3,5,13,20,22}. The literature primarily focuses on heterogeneous materials which are mixtures of two materials that each have different, isotropic electrical conductivities. The most well-known result is that of Maxwell, which is based on an effective-medium approximation for dilute suspensions¹⁵. Hashin and Shtrikman approached the problem in a different way. Rather than attempt to solve for an exact expression for the effective conductivity of a randomly structured material, they applied a variational method to derive upper and lower bounds on the effective conductivity¹⁰. They chose to use a variational approach to derive bounds on the conductivity because solving the exact problem for an arbitrarily structured heterogeneous material was analytically intractable. Torquato^{20–22} has studied the effective conductivity problem in great depth. He has improved the bounds laid out by Hashin and Shtrikman, has solved for effective conductivity of a number of different lattice types, and has expressed the exact tensorial effective conductivity in terms of an infinite series of N-point probability functions, which can be used to describe the microstructure of a heterogeneous material. The particular case of a suspension consisting of a conductive particle network within an insulating medium has been considered theoretically, to our knowledge, in one existing study¹³. The approach they take assumes a spatially homogeneous potential gradient field imposed upon the structure, leading to a model for the conductivity that can be proven to be an upper bound.

Much of the aforementioned work is concerned with the

isotropic conductivity of heterogeneous materials. In this work, we aim to model the full tensorial conductivity, with a focus on suspended networks of conductive particles. These particle networks are of practical importance, especially in flowable battery technology currently under development by the Joint Center for Energy Storage Research (JCESR)⁶. In these batteries, a conductive, flowing suspension of carbon black forms an integral component of the system, see Figure 1(a). It has been shown in related systems¹² that shearing flows induce anisotropy in a contact network of suspended particles, as pictured in Figure 1(b). In instances where suspension conductivity arises from particle-particle contacts, this structure anisotropy should give rise to conductivity anisotropy. It is this behavior that we seek to describe. It has been shown experimentally that the electrical conductivity of a suspension is highly sensitive to shear rate¹, dropping by several orders of magnitude as shear rate increases. From this observation and the evidence of particle microstructure changing in shearing flow, we deduce that a suitably chosen description of the particle network should be sufficient to predict the electrical conductivity of a suspension.

In the granular media literature, a great deal of attention has been given to describing the structure of the contact network between particles. Perhaps the simplest structural measure for such a network that includes anisotropy is the *fabric tensor*^{16,17,19}. While more complex structural measures exist, such as pair- and higher-order particle correlation functions²², whose use could enable greater accuracy in constructing a conductivity model, we shall show that a suitable model can be achieved solely in terms of the fabric. Key to our model development is the solution of a simple case, based on a network conforming to a lattice structure. The results instruct the form for a new conductivity model, whose accuracy is then tested

^{0a} Department of Mechanical Engineering, MIT, Cambridge, MA, USA.

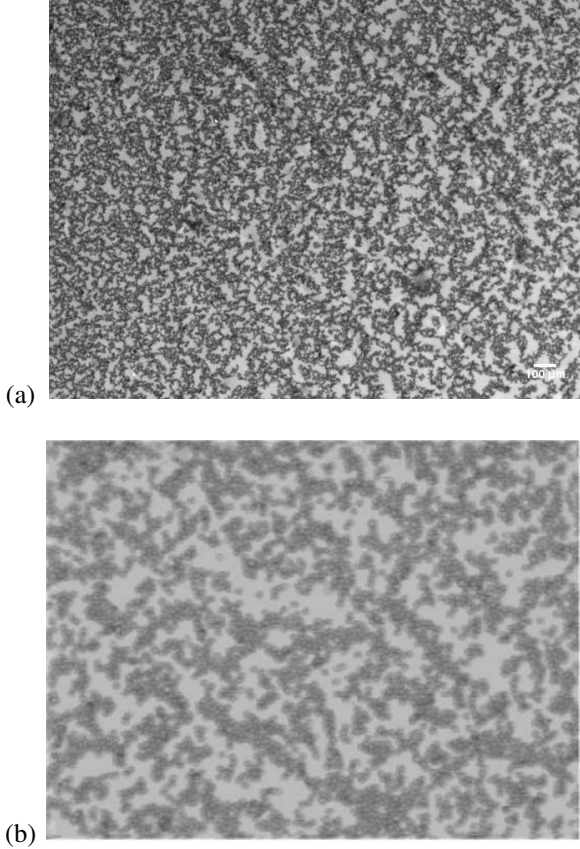


Fig. 1 (a) Image of a carbon black particle network, an electrically conductive suspension¹¹. (b) Image of an effective two-dimensional suspension (attractive polystyrene beads on a fluid surface), which has been subjected to shearing. Note the formation of an anisotropic contact network between particles.¹²

against many thousands of random particle networks. To explore a range of particle networks, we describe two distinct algorithms for creating random packings — one for denser packings, and one for more dilute packings that closely resemble those formed by carbon-black — and demonstrate the model’s predictive capability against thousands of packings generated from both algorithms.

Homogenization

The tensorial form of Ohm’s law relates the electric field vector \mathbf{E} to the current density vector \mathbf{J} through a second-order conductivity tensor \mathbf{K} , i.e.

$$\mathbf{J} = \mathbf{K}\mathbf{E} \quad (1)$$

The conductivity tensor is a symmetric, positive-definite tensor²¹. An effective conductivity for a representative volume

Ω of a heterogeneous material must be defined prior to any analytical or numerical work. The effective conductivity of an ergodic medium is defined by

$$\langle \mathbf{J} \rangle = \mathbf{K} \langle \mathbf{E} \rangle \quad (2)$$

where $\langle \mathbf{E} \rangle$ and $\langle \mathbf{J} \rangle$ are, respectively, the spatially-averaged electric and current density fields over Ω ²¹. To avoid a possibly over-reaching assumption of ergodicity — our tests will be conducted on finite domains — we specify that $\langle \mathbf{E} \rangle$ is imposed by prescribing a linear boundary potential $\varphi(\mathbf{x} \in \partial\Omega) = -\langle \mathbf{E} \rangle \cdot \mathbf{x}$, and that $\langle \mathbf{J} \rangle$ is redefined as the flux that is power-conjugate to $\langle \mathbf{E} \rangle$. That is,

$$\langle \mathbf{E} \rangle \cdot \langle \mathbf{J} \rangle \equiv \frac{1}{V} \int_{\Omega} -\nabla\varphi \cdot \mathbf{j} dV \quad (3)$$

where \mathbf{j} is the local current density field. In the ergodic limit of the ensuing analysis, $\langle \mathbf{J} \rangle$ reduces to a standard spatial average.

Assuming that the current density obeys Kirchoff’s current law and Ohm’s law — respectively, $\nabla \cdot \mathbf{j} = 0$ and $\mathbf{j} = -\sigma \nabla \varphi$ for some non-negative conductivity field $\sigma(\mathbf{x})$ — a symmetric, positive-definite conductivity tensor \mathbf{K} must exist that obeys (2). By using the divergence theorem, Eq 3 can be transformed into

$$\langle \mathbf{E} \rangle \cdot \mathbf{K} \langle \mathbf{E} \rangle = \frac{1}{V} \int_{\partial\Omega} -\varphi \mathbf{j} \cdot \mathbf{n} dA \quad (4)$$

where \mathbf{n} is the outward-pointing normal vector.

We model the particles as perfect conductors, the fluid as a perfect insulator, and we suppose electrical resistance arises only at the contacts between particles. Likewise, the field φ is approximated as a constant within each particle but possibly varying from particle to particle. The above integral can now be broken into a sum of integrals over the boundary. In the locations where the boundary passes through free space (i.e., not a particle), then we know that \mathbf{j} is exactly $\mathbf{0}$. This leaves only the parts of the boundary that pass through particles, which allows us to write the integral over the set of boundary particles B , i.e.

$$\langle \mathbf{E} \rangle \cdot \mathbf{K} \langle \mathbf{E} \rangle = \frac{1}{V} \sum_{i \in B} -\varphi_i \int_{\partial\Omega_i} \mathbf{j} \cdot \mathbf{n} dA. \quad (5)$$

where Ω_i is the intersection of the i th boundary particle with $\partial\Omega$, and the potential within particle i , denoted φ_i above, can be brought outside the integral since it is constant within a particle. Although the precise nature of \mathbf{j} is unknown within the particle, the value of the integral $\int_{\partial\Omega_i} \mathbf{j} \cdot \mathbf{n} dA$ is the current that is flowing out of Ω . Denoting this current as I_i^{out} we can write the final expression for the right-hand-side of (4),

$$\langle \mathbf{E} \rangle \cdot \mathbf{K} \langle \mathbf{E} \rangle = \frac{1}{V} \sum_{i \in B} -\varphi_i I_i^{out}. \quad (6)$$

The three independent components of \mathbf{K}_e can be determined by performing multiple simulations on the same particle network with three non-colinear choices of $\langle \mathbf{E} \rangle$.

By our assumptions for the particle properties, the problem can be reduced further to that of a resistor network. The network is defined by the set of particles acting as the nodes, which are connected by a set of contacts acting as the edges, which carry a resistance R_c . In our model development and simulations, we assume that R_c is a constant at all contacts. In reality, this is not strictly the case since the contact resistance is affected by the contact area between particles and the local structure of the network. This was studied in detail by Batchelor⁴. If the particles in question were Hertzian elastic spheres compressed into a dense granular packing, spatially-fluctuating contact forces arise causing fluctuating contact areas, and this issue may be a factor to consider. However, for the suspensions of interest in this study, the particles actually have an open, fractal structure, and form contacts only due to van der Waals attraction. Absent any information to inform the size of the contact area beside the \sim constant attractive force, we choose to use a constant contact resistance. A schematic of an example network with 9 nodes and 12 edges can be found in figure 2. Supposing an N -particle sample and letting $i_{m,n}$ represent the (signed) current flowing from particle m to n , Ohm's and Kirchoff's law can be rewritten in their simpler discrete form,

$$i_{m,n} = \frac{\varphi_m - \varphi_n}{R_c} H_{mn} \quad (7)$$

and

$$\sum_n i_{m,n} = 0 \text{ for all } m. \quad (8)$$

where H_{mn} is the adjacency matrix of the graph formed by the particle network. $H_{mn} = 1$ if there is an edge connecting particles m and n , and zero otherwise. These equations define a sparse linear system that can be solved for the potential at each particle after applying appropriate boundary conditions, which is described in a later section. The resulting linear system is sparse, symmetric, and positive definite, so we used a sparse Cholesky direct solver to compute the potential at each point. A trivial post-processing step can be performed to compute the current through each contact.

Solving these linear equations for a given particle network enables us to calculate I^{out} in (6) and hence the conductivity tensor for the network.

We choose to use the fabric tensor as the measure of the network structure. The particle-level fabric is a local quantity that can be defined for particle p by the relation^{16,17,19}

$$\mathbf{A}^p = \sum_i \mathbf{n}_i \otimes \mathbf{n}_i \quad (9)$$

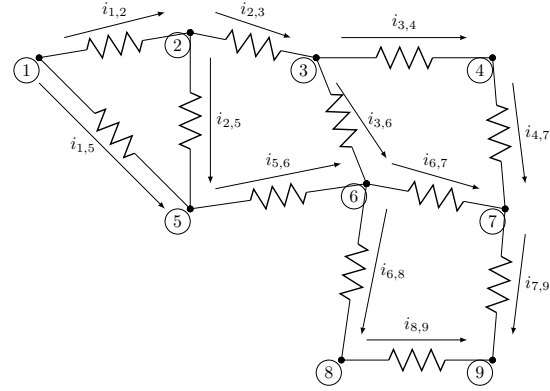


Fig. 2 Schematic of a small resistor network with nodes and edges labeled according to our conventions.

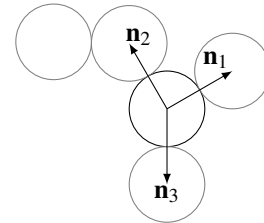


Fig. 3 Schematic of particles in contact showing contact vectors \mathbf{n}_i .

where \otimes denotes the dyadic product, and \mathbf{n}_i is the unit vector connecting particle centroids of the i 'th contact on the particle. This is illustrated in Figure 3. To homogenize over the entire particle network, or at least meso-sized region of it, the average fabric tensor is defined as the system average of the particle fabric tensors.

$$\mathbf{A} = \frac{1}{N_{\text{particles}}} \sum_{p=1}^{N_{\text{particles}}} \mathbf{A}^p \quad (10)$$

The definition of the fabric tensor has some attractive features. It is symmetric and positive-semidefinite, guaranteeing that the eigenvalues are non-negative and that the eigenvectors are orthogonal. These properties are shared by the conductivity tensor \mathbf{K} , suggesting the fabric tensor could be an appropriate independent variable in the conductivity's functional form.

An important concept that will be used later is that of a tensor deviator. The tensor deviator is the trace-free part of a tensor, and it is useful to describe anisotropic phenomena since it has the isotropic part removed. It is defined as

$$\mathbf{A}_0 = \mathbf{A} - \frac{1}{d} \text{tr} \mathbf{A} \mathbf{1} \quad (11)$$

where d is the spatial dimension and $\mathbf{1}$ is the identity tensor.

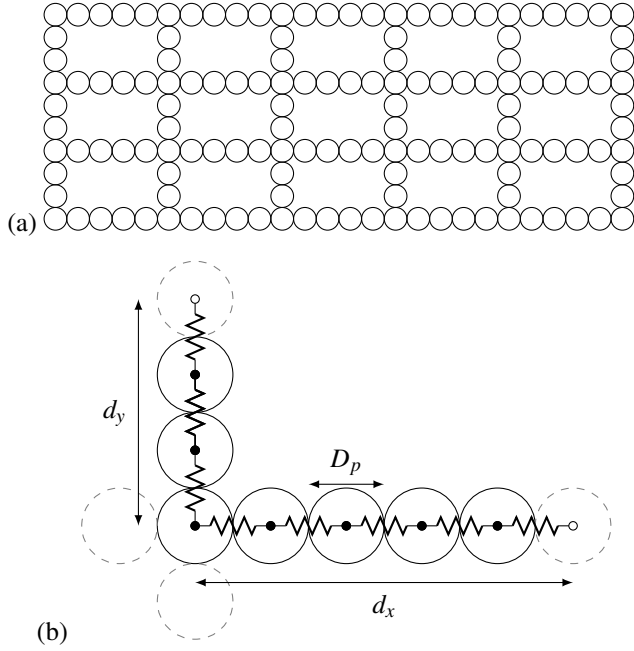


Fig. 4 Idealized particle lattice and unit cell from which fabric-conductivity relation was derived. (a) Example 2D idealized particle lattice. (b) 2D lattice unit cell and its resistor network analog. Neighboring unit cells are shown in gray dashed lines.

Lattice-Reduced Model

We propose an analytical model to elucidate the connection between electrical conductivity and the fabric tensor based on a simplified lattice structure. We will test this model's applicability to random packings in the later sections.

The particles are imagined to live on an idealized infinite, periodic lattice. The lattice is parameterized by a set of numbers that describe the particle size and spacing. These parameters are (1) particle diameter D_p , (2) distance in x-direction between chains d_x , (3) distance in y-direction between chains d_y , (4) distance in z-direction between chains d_z . In 2D, only the first three parameters are used. An illustration of a 2D lattice characterized by these parameters is shown in figure 4(a), with its fundamental unit cell shown in figure 4(b).

Both the average fabric tensor and effective conductivity can be computed analytically. The average fabric tensor is defined as the spatial average of the fabric tensor for all of the particles in the unit cell and ultimately results in the formula

$$\mathbf{A} = \frac{2}{N_x + N_y - 1} \begin{bmatrix} N_x & 0 \\ 0 & N_y \end{bmatrix} \quad (12)$$

In this expression, the key quantities to recognize are the number of particles in the x-oriented chain, $N_x = d_x/D_p$, and the

number of particles in the y-oriented chain, $N_y = d_y/D_p$.

Next, the effective conductivity was derived for the unit cell. To do this, imagine applying an arbitrary voltage difference across the x-oriented and y-oriented chains separately. These voltages are $\Delta\phi_x$ and $\Delta\phi_y$, respectively. By applying Ohm's law through the corresponding chains, we can recover the components of the vector form of Ohm's Law shown in (1). For example, for the x-oriented chain

$$j_x = \left(\frac{1}{N_y R_c} \right) (\nabla\phi)_x \quad (13)$$

with $(\nabla\phi)_x = \Delta\phi_x/d_x$. Due to the geometry of the problem, we know that the off-diagonal components of the conductivity tensor \mathbf{K} are exactly zero. Therefore, we can say

$$K_{11} = \frac{1}{N_y R_c}. \quad (14)$$

Similarly analysis yields

$$K_{22} = \frac{1}{N_x R_c}. \quad (15)$$

Finally, the parameters N_x and N_y can be algebraically eliminated to give the components of \mathbf{K} in terms of the components of \mathbf{A} , yielding the tensorial relationship

$$\mathbf{K} = \frac{1}{R_c} \frac{\text{tr}\mathbf{A} - 2}{\det\mathbf{A}} \mathbf{A}. \quad (16)$$

We refer to the formula in (16) as the "lattice model". A similar analysis can be carried out for a three-dimensional unit cell, which will yield the following expression for the conductivity tensor,

$$\mathbf{K} = \frac{1}{4D_p R_c} \frac{(\text{tr}\mathbf{A} - 2)^2}{\det\mathbf{A}} \mathbf{A}. \quad (17)$$

The formulae above apply when $\text{tr}\mathbf{A} - 2$ is non-negative. Otherwise the solution is $\mathbf{K} = \mathbf{0}$. The matrix $\mathbf{A}/\det\mathbf{A}$ can be understood as an approximate measure of how much a lattice cell of given perimeter (area) deviates from a square (cube) configuration, distributing proportionally less conductivity in directions where particle chains are more separated and more conductivity in directions where chains are tightly spaced.

Despite its inspiration from the lattice structure, there are several reasons to consider the applicability of the lattice model to more general particle networks. For one, the formula purports codirectionality of the fabric and conductivity, i.e. the deviators of the two tensors are aligned, implying that the direction of anisotropy of one tensor gives the anisotropy direction of the other, which to a first approximation ought to match the behavior of general particle networks. Second, the results imply that conductivity should vanish when $\text{tr}\mathbf{A} < 2$,

which is sensible more generally (though not strictly) because particles in a percolating chain, as needed to conduct current across the sample, must have coordination number at least two. Above this threshold, conductivity increases with $\text{tr}\mathbf{A}$ in line with one's basic intuition for more highly coordinated networks. In reality, islands of monomers, dimers, etc, enable the possibility of conductivity with an average coordination number less than two because conductivity will be nonzero with any percolating chain of particles. However, the geometric assumption underlying this lattice model prevents this from being taken into consideration. This shortcoming of the model is evident in our numerical results in figure 8 where nonzero conductivity was observed for a small range of coordination numbers below two.

We are aware of one other fabric-based analytical model for conductive particle networks, which was developed by Jagota and Hui¹³. In their work, a uniformity hypothesis is made with regard to the potential gradient, which results in a conductivity model that is fully linear in the fabric tensor,

$$\mathbf{K} = \frac{N_V D_p^2}{2R_c} \mathbf{A}. \quad (18)$$

The above, which can be proven to be an upper-bound on the real conductivity, is for a two-dimensional system and N_V is the particle number fraction (per area in 2D). In the isotropic case, (18) reduces to precisely the Hashin-Shtrikman upper bound one finds for the limit of thin, conductive bridges (of net resistance R_c) connecting the centers of contacting particles^{10,21}. The above model differs from ours most notably in that the conductivity is not thresholded by the coordination number, the formula depends explicitly on the particle area fraction as well fabric, and it does not depend on the fabric determinant.

Numerical Simulation

In order to perform numerical experiments and determine the generality of the lattice model, a large number of random particle networks (packings) must be created. There are a number of methods to do this already in the granular and particulate matter literature. See the references for a broad summary of the currently available granular packing algorithms². Attractive suspensions have been modeled with the Diffusion-Limited Aggregation (DLA) model of Witten and Sander¹⁴. A common feature of many of the granular statics methods is that they solve force equilibrium equations for a system of particles. This was not a feature that was required for this study, so these types of methods were not used, in the interest of saving computational time. Instead, we developed two methods for creating two-dimensional random contact networks of

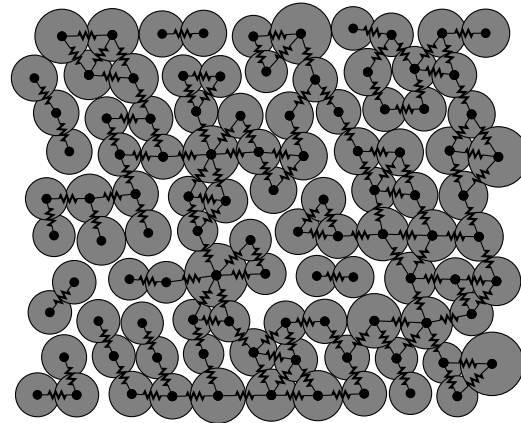


Fig. 5 Example (using a small number of particles) of a dense particle packing resulting from Algorithm 1.

particles, and we tested our model against numerous packings generated by each method. Both methods allow us to influence the resulting anisotropic structure of the packings.

Algorithm 1: Our first packing algorithm was designed to create a dense random contact networks of particles. This is in contrast to a later algorithm, to be described below, which created packings that resulted in much lower-density packings. The dense packings were created by perturbing a 2D hexagonal close-packing of particles. This was achieved by placing points into a triangular lattice, adding random noise to the position of each point, and finally growing each particle as large as possible such that no particles overlapped. Anisotropy can be influenced by shearing the points with an affine transformation $\mathbf{x}' = \mathbf{F}\mathbf{x}$ before growing the radii. This process is described in pseudocode below (Algorithm 1). An example of the resulting packing overlaid by its analogous resistor network is shown in figure 5.

Algorithm 1

```
Seed  $L \times L$  box with close-packed points
Perturb points with random noise
Move each point to new location  $\mathbf{x}'$  by  $\mathbf{x}' = \mathbf{F}\mathbf{x}$ 
while Not all radii frozen do
  Find smallest distance that any particle can grow
  Grow all particles by this amount
  Freeze radii of particles that come into contact
end while
```

Algorithm 2: This procedure was motivated by a need to better understand the conductivity of carbon black suspensions in an insulating medium. The self-attraction carbon black particles leads to fractal particle networks that are electrically percolating at low volume fraction (below 1 vol%)⁶.

Algorithm 2

```

Seed N clusters (particles) in  $L^d$  square
while  $N_{clusters} > 1$  do
  Move clusters according to  $\mathbf{v} = -\mathbf{B}(\mathbf{x} - \mathbf{O})$ 
  Locate collisions between clusters
  Combine clusters in contact and recompute centroids
end while

```

To produce structures that more closely resemble carbon black suspensions, we developed our second packing algorithm, which is inspired by the “hit-and-stick” behavior of the carbon particles. In addition, the new algorithm is able to include the effects of particle Brownian motion but this is not essential to the algorithm.

First, clusters (single particles at this stage) are seeded randomly into a L^d box, where d is the number of spatial dimensions. Next, a linear velocity field is imposed directly on each cluster’s centroid according to

$$\mathbf{v} = -\mathbf{B}(\mathbf{x} - \mathbf{O}) \quad (19)$$

where \mathbf{O} is a point in the middle of the original box. This imposed velocity field serves to pull all of the clusters together. The matrix \mathbf{B} is a $d \times d$ matrix that allows us to impose an anisotropic velocity field. This allows us to influence (but not completely impose) the fabric tensor that results from this packing method. After the velocity field is imposed, the particle positions are updated by assuming a time step dt (computed at runtime). Then, the clusters are checked to determine whether any contacts have been made with other clusters. If so, the clusters are cohered into a single cluster for all future steps. This process of imposing velocity, updating positions, and handling contacts is repeated until only a single cluster remains. The process is outlined in pseudocode in Algorithm 2. An example of a packing resulting from this process is shown in figure 6 and a larger example is displayed in figure 7.

The box-counting fractal dimension⁷ of the resulting packings was computed in order to determine if they resembled real-life packings found in experiments. The fractal dimension of packings produced by this method is approximately $d = 1.75$. This was compared against the particle network image in figure 1. This network has a fractal dimension of approximately $d = 1.7 \pm 0.1$. Uncertainty in the measurement is due to the image processing techniques used to identify particles. Based on these measurements, we are satisfied that this algorithm produces realistic packings, although more detailed correlation function measurements would be needed for a firmer conclusion.

Applying boundary conditions: In order to apply the solution method described above to an arbitrary packing of particles,

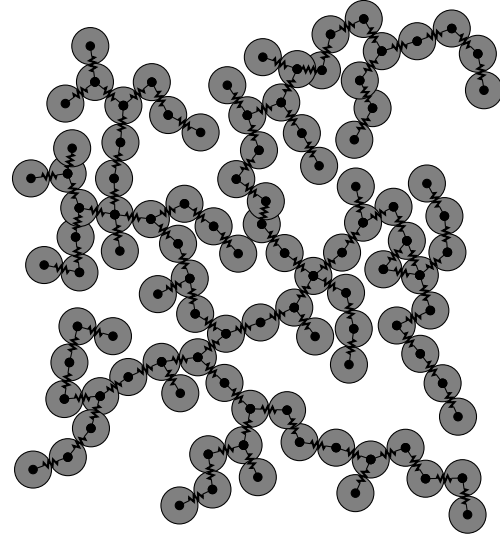


Fig. 6 Example (using a small number of particles) of a packing resulting from Algorithm 2 using a small number of particles.

appropriate boundary conditions must be applied. In these simulations, a prescribed voltage was applied to particles all around the boundary. This process consists of two steps: first, the boundary must be identified, and second, the linear system must be updated to reflect the known voltages.

For the first packing algorithm, identifying the boundary is a trivial process, since the particle locations are known a priori. For algorithm 2, however, the particle positions are not known. A boundary can be located visually quite easily at the end of the simulation process, but performing this step manually would be prohibitively slow. In order to expedite and automate the simulation process, the following method was devised to locate the boundary.

First, histograms of the particle x and y positions were separately created. To find the “left” and “right” boundaries, denoted x^- and x^+ respectively, the histogram of x positions was thresholded. The value x^- is defined as the smallest x value where the histogram reaches 50% of its maximum value. The value x^+ is defined as the largest x value that meets the same criterion. The top and bottom boundaries, y^+ and y^- , are found in the same manner using the histogram of particle y coordinates. The threshold value 50% was determined empirically to locate the same boundary that one would identify visually. An example packing and its associated x -position histogram is shown below in figure 7 to demonstrate the efficacy of the method. Once the location of the boundary has been identified, all particles whose centers fall less than one radius away from the lines are marked as being “boundary particles”.

The expression in (6) can be computed easily from the solu-

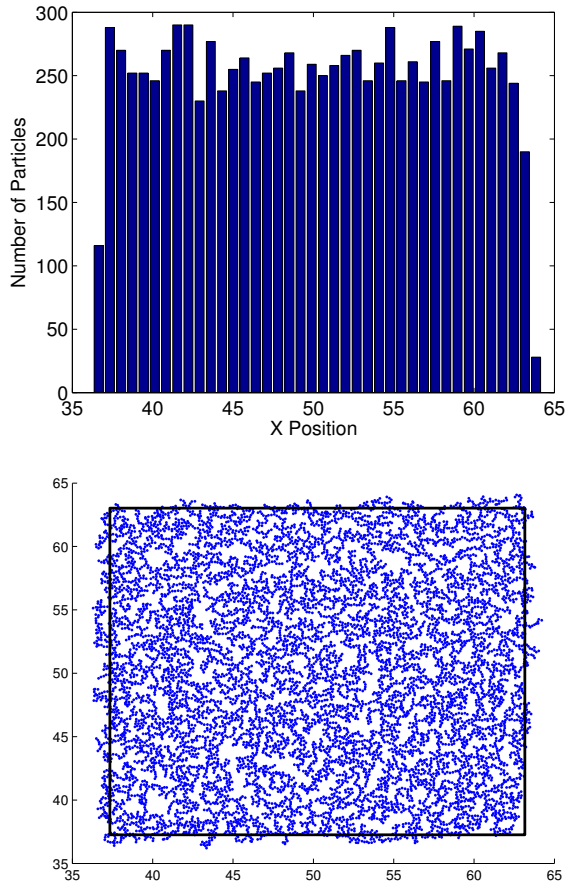


Fig. 7 Example 10,000-particle packing (from Algorithm 2) with its associated x-position histogram and the boundary selected by the method.

tion of the particle network, so by judiciously choosing $\langle \mathbf{E} \rangle$, the components of \mathbf{K}_e can be extracted. In two dimensions, the effective conductivity tensor has three independent components, so three simulations are sufficient to extract all of the components. The K_{11} component can be extracted by setting $\langle \mathbf{E} \rangle = \mathbf{e}_x$. This corresponds to evaluating the integral for an applied boundary voltage of $\varphi = -x$. The remaining tensor components may be similarly extracted by applying specific potential fields at the boundary and evaluating the summation given in (6).

Tests

The previously described packing algorithms and solution procedures for the current/potential have been implemented in Matlab. Algorithm 1 was used to create 50,000 separate 400-particle packings. In all of these packings, the F_{11} and

F_{22} components of the affine transformation \mathbf{F} equalled 1.0. The F_{12} component that controlled the shearing of the packing ranged between 0 and 0.5 in increments of 0.01. Any particles that were sheared out of the original bounding rectangle were reflected to the other side of the box to return the packing to a rectangular geometry. We find packing fractions in the range $\phi \in [0.65, 0.80]$. Algorithm 2 was used to create 10,000 separate 5,000-particle packings. In the \mathbf{B} matrix, the B_{11} component remained 1.0, and the B_{22} component was varied in $[1.0, 1.9]$ in increments of 0.1 to influence the level of anisotropy of the resulting packings. The approximate range of packing fractions we find is $\phi \in [0.45, 0.70]$. After applying the previously described procedure to each packing to obtain the effective conductivity tensor and average fabric tensor for each packing, the data were analyzed to determine how well the results agree with the model's predictions for the isotropic magnitude, the deviatoric magnitude, and the direction of conductivity. If the model is successful, then for any choice of \mathbf{A} , the model should match the ensemble average conductivity of all packings having that fabric \mathbf{A} . Below, for ease of demonstration, we bin the data based on scalar invariants of \mathbf{A} , and show either the ensemble average of the conductivity data at different choices of those scalars, or simply show scatter-plot comparisons against the full set of tests when it is more illustrative to do so. These tests are described next, and thereafter we shall proceed to show how well the lattice model performs compared to the existing model, equation (18).

The isotropic behavior of the conductivity can be investigated by taking the trace of both sides of (16). The average coordination number is the most natural independent variable when examining the isotropic behavior, so in addition to taking the trace of both sides of (16), both sides were multiplied by $\det \mathbf{A}$ in order to make the right-hand side a single-valued function of $\text{tr} \mathbf{A}$. This results in (20).

$$R_c \text{tr} \mathbf{K} \det \mathbf{A} = (\text{tr} \mathbf{A} - 2) \text{tr} \mathbf{A} \quad (20)$$

The results of the simulations are scatter-plotted together with the analytical curve given by (20) in figure 8. It was found that the analytical solution is usually an upper bound on the measured conductivity. This can be explained by the fact that the analytical model was derived from an idealized system where the chains span a unit cell in a straight line. Since the total resistance of a chain is proportional to the number of contacts in the chain, it follows that the shortest chain between any two points is the lowest resistance path, and therefore most conductive. Since the model was derived from a straight-chain idealization, it implies an upper bound on the conductivity. This logic is less valid in low-coordinated systems, which have many disconnected groupings of one or two particles; low-coordinated systems rarely if ever occur from Algorithm 2 or

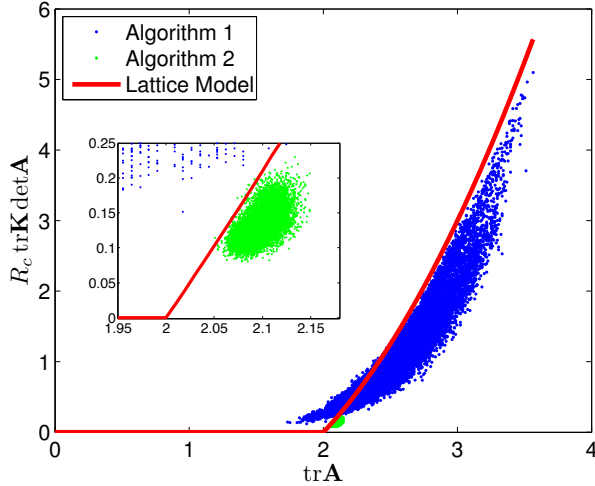


Fig. 8 Predicted relationship between the (modified) trace of the conductivity and the fabric trace, compared to numerical results of 50,000 packings generated by Algorithm 1 and 10,000 generated under Algorithm 2. Inset is a zoom-in of the vicinity of $\text{tr} \mathbf{A} = 2$.

in actual carbon black suspension networks. In this case, the trace of the system's fabric can be less than 2 but percolating chains may still exist to produce small but non-zero conductivity. This effect is evident in the figure in the data of Algorithm 1.

Next, we determine the extent the analytical lattice model predicts the anisotropy of the conductivity. To remove the influence of the isotropic behavior, we take the deviator of both sides of (16). In this case, the most natural independent variable is the magnitude of the fabric deviator, so the resulting equation was manipulated to be a single-valued function of this quantity. After manipulation, (16) can be written as (21).

$$R_c \mathbf{K}_0 : \frac{\mathbf{A}_0}{|\mathbf{A}_0|} \left(\frac{\det \mathbf{A}}{\text{tr} \mathbf{A} - 2} \right) = |\mathbf{A}_0| \quad (21)$$

where a subscript 0 denotes the deviator of the tensor, and the term $\frac{\mathbf{A}_0}{|\mathbf{A}_0|}$ is commonly referred to as the direction or sign of the tensor \mathbf{A}_0 . The left hand side was plotted against $|\mathbf{A}_0|$ by binning all the test data by $|\mathbf{A}_0|$ and ensemble averaging in each bin. It can be seen in figure 9 that, although there is a large amount of noise in the measurements, the model captures the average behavior very closely.

The final prediction that must be examined is the notion of codirectionality. The analytical model in (16) predicts that the fabric and conductivity tensors have the same eigenvectors. To examine this, the angle difference between the fabric and conductivity deviators was calculated, which is equivalent to the (signed) angle between the eigenvectors corresponding to the largest eigenvalues of the two tensors, denoted \mathbf{e}_K and

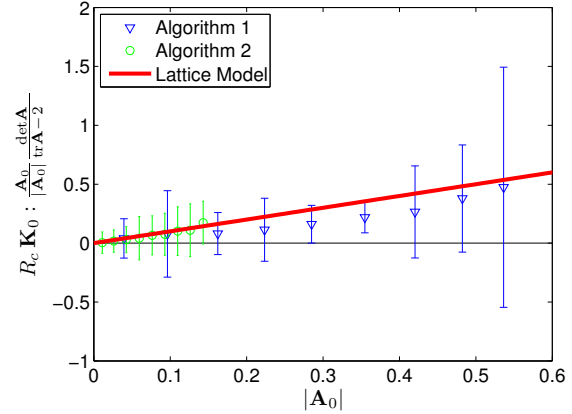


Fig. 9 Predicted relationship between effective magnitude of the anisotropy of the conductivity and the invariants of the fabric. Error bars show \pm one standard deviation.

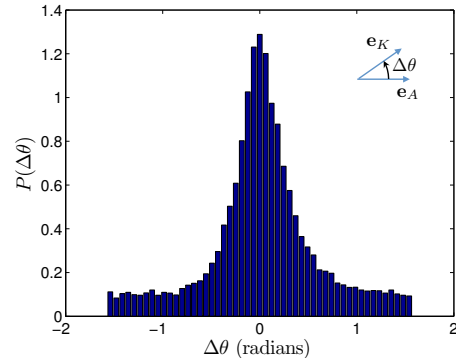


Fig. 10 PDF of angle differences are distributed around zero, indicating codirectionality of the fabric and conductivity tensors, as predicted by the analytical model, i.e. (16).

\mathbf{e}_A . The deviators were chosen because, in 2D, the eigenvector corresponding to the positive eigenvalue can be unambiguously chosen. The probability density function of the angle difference as a function of $\Delta\theta$ is plotted in figure 10. It can be seen that this distribution is symmetrically centered around zero, indicating that the fabric and conductivity are strongly codirectional.

Finally, we also compared the lattice model, (16), to the existing model by Jagota & Hui¹³ shown in (18). For the same 60,000 packings generated using both packing algorithms, we computed the relative error of the prediction of the trace and the determinant of the conductivity using each model and plotted the results in figures 11 and 12. In every case, we found that the new lattice model predictions were closer to the true values from the numerical experiments than the previous model by Jagota & Hui. On the other hand, the Jagota & Hui model maintains a strong upper bound on both invari-

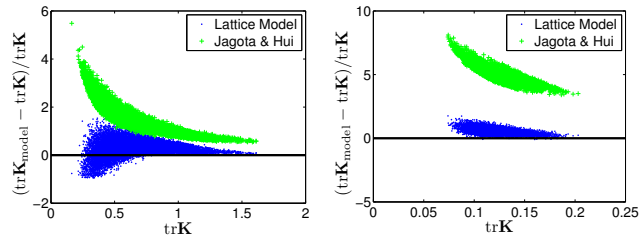


Fig. 11 Plot of the relative error of the trace of conductivity. (Left) Relative error from packings created with Algorithm 1. (Right) Relative error from packings created with Algorithm 2.

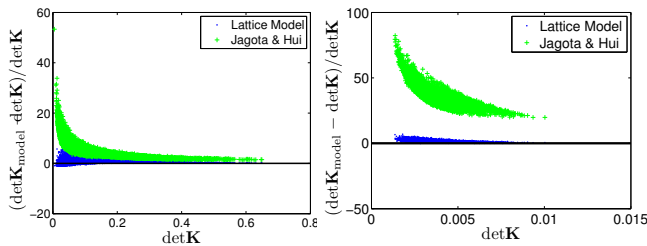


Fig. 12 Plot of the relative error of the determinant of conductivity. (Left) Relative error from packings created with Algorithm 1. (Right) Relative error from packings created with Algorithm 2.

ants of the conductivity tensor, whereas the lattice model is not strictly an upper bound, as previously discussed. In addition, since the isotropic part of the Jagota & Hui model is identical to the Hashin-Shtrikman upper bound on conductivity, Figure 11 also indicates that the Lattice Model is falling within this bound. To be more precise, the lattice model prediction for the isotropic part of conductivity is always less than the Hashin-Shtrikman upper bound computed for a given packing.

Discussion and Conclusions

In this paper we have derived and tested a new model relating the structure of a packing of particles to its tensorial electrical conductivity. The assumptions implicit in the model are that the suspending medium is a perfect insulator and that electrical resistance arises only at particle contacts. The structural measurement used was the fabric tensor, and the model arises from a straightforward analysis of a representative problem involving a lattice structure. The resulting model takes a non-linear functional form, and was tested multiple ways against numerical simulations of many thousands of random particle packings. The agreement in its predictions of the various scalar properties and tensorial orientation is significant, especially in light of the simplistic nature of the fabric tensor being the sole independent variable for the model. In our tests, the

lattice model's accuracy was shown to be higher than an existing conductivity model, a model which requires more structural input data than the lattice model. While it is definitely possible to write a more accurate model by including dependences on more structural variables — some of our data spread is due to the finite nature of the datasets, but some is surely due to modeling error — the current simplicity of the lattice model is an advantage for its usage in engineering applications involving flowing suspension networks. Modeling frameworks for the evolution of anisotropy tensors in flowing media have been developed over the last decades^{8,9,18}; keeping our model in terms of fabric, then, suggests a path to the simulation of simultaneous flow and current transfer fields in nontrivial systems by coupling a fabric evolution rule and a rheology with our conductivity model. Such a capability would be key in the targeted application of modeling flow battery systems, which rely on a flowing conductive suspension that closely resembles the idealized system that we considered. A second direction for future work would be to apply the same idea of simultaneous flow and anisotropy modeling to other transport phenomena. For example, incompressible flow through a deforming granular media would have a similar mathematical formulation, albeit with reversed spatial assumptions since the impermeable grains play the role of the insulating medium here. The fabric tensor could be used as a surrogate to describe the structure of the pore space, which would relate to anisotropic permeability.

Acknowledgements

The authors acknowledge support from the Joint Center for Energy Storage Research (JCESR), an Energy Innovation Hub funded by the U.S. Department of Energy, Office of Science, Basic Energy Science (BES). The authors declare that there are no conflicts of interest.

References

- 1 Takeshi Amari. Flow properties and electrical conductivity of carbon black/linseed oil suspension. *Journal of Rheology*, 34(2):207, February 1990.
- 2 Katalin Bagi. An algorithm to generate random dense arrangements for discrete element simulations of granular assemblies. *Granular Matter*, 7(1):31–43, January 2005.
- 3 GK Batchelor. Transport properties of two-phase materials with random structure. *Annual Review of Fluid Mechanics*, 1974.
- 4 GK Batchelor and RW O'Brien. Thermal or electrical conduction through a granular material. *...of the Royal ...*, 1977.

REFERENCES

REFERENCES

- 5 H. Cheng and S. Torquato. Effective conductivity of periodic arrays of spheres with interfacial resistance. Proceedings of the Royal Society A: Mathematical, Physical and Engineering Sciences, 453(1956):145–161, January 1997.
- 6 Mihai Duduta, Bryan Ho, Vanessa C. Wood, Pimpa Limthongkul, Victor E. Brunini, W. Craig Carter, and Yet-Ming Chiang. Semi-Solid Lithium Rechargeable Flow Battery. Advanced Energy Materials, 1(4):511–516, July 2011.
- 7 Kenneth Falconer. Fractal geometry: mathematical foundations and applications. John Wiley & Sons, 2013.
- 8 Charles O Frederick and PJ Armstrong. A mathematical representation of the multiaxial baushinger effect. Materials at High Temperatures, 24(1):1–26, 2007.
- 9 George L Hand. A theory of anisotropic fluids. Journal of Fluid Mechanics, 13(01):33–46, 1962.
- 10 Z. Hashin and S. Shtrikman. A Variational Approach to the Theory of the Effective Magnetic Permeability of Multiphase Materials. Journal of Applied Physics, 33(10):3125, 1962.
- 11 Ahmed Helal, Kyle Smith, Frank Fan, Xin Wei Chen, Joao Miguel Nobrega, Yet-Ming Chiang, and Gareth H. McKinley. Study of the rheology and wall slip of carbon black suspensions for semi-solid flow batteries. The Society of Rheology 86th Annual Meeting, October 2014.
- 12 H Hoekstra, J Vermant, J Mewis, and GG Fuller. Flow-induced anisotropy and reversible aggregation in two-dimensional suspensions. Langmuir, (11):9134–9141, 2003.
- 13 A Jagota and C Y Hui. The Effective Thermal Conductivity of a Packing of Spheres. J. Appl. Mech., (September 1990):789–791, 1990.
- 14 TA Witten Jr and LM Sander. Diffusion-limited aggregation, a kinetic critical phenomenon. Physical review letters, 47(19), 1981.
- 15 James Clerk Maxwell. A treatise on electricity and magnetism, volume 1. Clarendon press, 1881.
- 16 Morteza M. Mehrabadi, S Nemat-Nasser, and M Oda. On statistical description of stress and fabric in granular materials. International Journal for ..., 6(November 1980):95–108, 1982.
- 17 M Oda, S Nemat-Nasser, and Morteza M. Mehrabadi. A statistical study of fabric in a random assembly of spherical granules. International Journal for Numerical and Analytical Methods in Geomechanics, 6(July 1982):77–94, 1982.
- 18 F. Radjai, J.-Y. Delenne, E. Azéma, and S. Roux. Fabric evolution and accessible geometrical states in granular materials. Granular Matter, 14(2):259–264, March 2012.
- 19 M Satake. Constitution of mechanics of granular materials through the graph theory. Continuum Mechanical and Statistical Approaches in the Mechanics of Granular Materials, pages 47–62, 1978.
- 20 S. Torquato. Effective electrical conductivity of two-phase disordered composite media. Journal of Applied Physics, 79(10(November)):3790–3797, 1985.
- 21 S. Torquato. Random heterogeneous materials: microstructure and macroscopic properties, volume 16. Springer, 2002.
- 22 S. Torquato and G. Stell. Microstructure of two-phase random media. I. The n-point probability functions. The Journal of Chemical Physics, 77(4):2071, 1982.